Progress In Electromagnetics Research M, Vol. 36, 139–147, 2014

Fast Wideband Analysis of Antennas Using IE-PO Hybrid Method and the Best Uniform Approximation

Wen-Feng Chen, Shu-Xi Gong*, Bo Zhao, and Peng-Fei Zhang

Abstract—An efficient wide-band analysis that combines modified integral equation-physical optics (IE-PO) hybrid formulation with the best uniform approximation is proposed for antennas around an electrically large platform in this paper. The modified single-level Fast Fourier Transform (FFT) algorithm which is based on the subdomain FFT acceleration is employed by interpolating the Green's function and introducing the concept of the empty groups. Furthermore, the correction of the near-interaction is avoided. On the other hand, the best uniform approximation technique is applied to analyze wide-band properties of antennas. Due to the above modifications, the hybrid method needs fewer unknowns and memory requirements than the conventional one.

1. INTRODUCTION

Usually a platform structure can significantly affect antenna properties in mobile communication, so existent mutual electromagnetic coupling effects should be well handled via numerical technique with low computational cost. As we know, the integral equation (IE) [1–3] method is very popular in solving electromagnetic problems.

In recent years, a series of classic fast IE methods have been proposed. Multilevel fast multipole algorithm (MLFMA) [4, 5] is an extension of fast multipole method (FMM) [6–8]. On the other hand, the researches of fast Fourier transform (FFT) based on grid basis function lead to more tractable methods, such as precorrected-FFT (P-FFT) [9, 10], conjugate gradient-FFT and adaptive integral method (AIM) [11]. In this class of approaches, the polynomial interpolation of the Green's function via uniform Cartesian grid brings forth a Toeplitz matrix, allows the fast computation of well-separated MoM interaction terms with the aid of a global FFT and is easier to implement than other approaches. As References [11–13] point out, the conventional MoM requires $O(N^2)$ for both storage and matrix-vector multiplication, where N denotes the number of unknowns. However, the FFT approach is $O(N^{1.5})$ for storage requirement and $O(N^{1.5} \log N)$ for matrix-vector multiplication for 3-D PEC electromagnetic problems.

However, for electrically large platform, the efficiency of IE method may be lost due to excessive computer requirement. It should be noted that the most powerful tool for solving such model is the hybrid algorithm which combines IE with high frequency asymptotic method. In the hybrid analysis, the original model is divided to the full-wave region and the asymptotic region, respectively. The interaction between two regions is accounted for in the integral equation (IE) resulting in that the unknowns only appears in the full-wave region. With the development in recent years, the hybrid approach shows the accuracy and validity of offering considerable computational saving in terms of memory and execution time.

In practical applications, the properties of antennas over a wide frequency band are usually concerned. With the hybrid algorithm, it is still time-consuming due to the repeated solution of

Received 31 March 2014, Accepted 16 May 2014, Scheduled 23 May 2014

* Corresponding author: Shu-Xi Gong (shxgong@163.com).

The authors are with the Science and Technology on Antennas and Microwaves, Xidian University, Xi'an, Shaanxi 710071, People's Republic of China.

matrix equation at each frequency point. Over the past few years, there have been some efforts to achieve fast frequency sweep, such as impedance matrix interpolation, asymptotic waveform evaluation (AWE) [14–18], model-based parameter estimation (MBPE) [19] and the best uniform approximation technique [20–22]. In AWE and MBPE, Taylor series expansion is generated for a specific value of the system parameter, and the rational function approach obtained from Padé approximation is used to improve the accuracy of the numerical solution. However, the accuracy of the Taylor series is limited by the radius of convergence, and the high derivatives of the dense impedance matrix must be stored to compute the coefficients, which will greatly increase the memory consumed. Compared with AWE and MBPE, the best uniform approximation is easy to be applied in IE method and can obtain accurate results over a wide frequency band without increasing memory.

In this paper, an improved IE-FFT approach combined with physical optics (PO) is utilized to analyze the radiation of antennas around an electrically large platform. By interpolating the Green's function and introducing the concept of the empty groups, the modified single-level Fast Fourier Transform (FFT) algorithm based on the subdomain can avoid the calculation process of near-interaction. Furthermore, the best uniform approximation technique is applied to get an accurate representation of the frequency response. Finally, numerical results show the efficiency of the approach proposed in this paper.

This paper is organized as follows. Section 2 gives a brief overview of the IEFFT-PO method, and then derives the best uniform approximation technique in detail. Two numerical examples will be presented in Section 3 to demonstrate the accuracy and efficiency of the hybrid technique. Finally, the conclusions and discussions will be provided in Section 4.

2. METHOD DESCRIPTION

2.1. The Combined Field Integral Equation

The CFIE is merely a linear combination of the EFIE and the MFIE as follows:

$$\text{CFIE} = \alpha\text{EFIE} + \frac{(1-\alpha)}{jk_0}\text{MFIE} \tag{1}$$

where α is the combination factor and $0 \leq \alpha \leq 1$. Note that the choice of the combination factor strongly depends on the accuracy and efficiency required. The larger the factor is, the more accurate the results are. In contrast, the smaller the factor is, the higher the efficiency is. It is found that combination factor $\alpha = 0.8$ is an overall good choice in Ref. [12].

After applying the conventional integral equation-physical optics (IE-PO) hybrid method, the CFIE can be converted into a matrix equation

$$(\mathbf{Z}_{11} + \mathbf{Z}_{12}\mathbf{A})\,\mathbf{I}_1 = \mathbf{V}_1 \tag{2}$$

$$\mathbf{I}_2 = \mathbf{A}\mathbf{I}_1 \tag{3}$$

where the sub-matrix $\mathbf{Z}_{11}$ and $\mathbf{Z}_{12}$ represent the self-interaction and mutual-interaction between the full-wave region and the asymptotic region; $\mathbf{A}$ is the matrix relating the electric current in the asymptotic region to the full-wave region; $\mathbf{I}_1$ and $\mathbf{I}_2$ are the current coefficient vector of the two regions, respectively.

In Equation (3), the elements of $\mathbf{A}$ can be written as:

$$\mathbf{A} = \delta \int_{T_n^+ + T_n^-} \left\{ \left[\left(\hat{t}_q^+ + \hat{t}_q^-\right) \cdot \nabla G\left(\mathbf{r}, \mathbf{r}'\right) \right] \hat{n}_q - \left[\hat{n}_q \cdot \nabla G\left(\mathbf{r}, \mathbf{r}'\right) \right] \left(\hat{t}_q^+ + \hat{t}_q^-\right) \right\} \cdot f_n(\mathbf{r}') d\mathbf{r}' \tag{4}$$

where $\hat{n}_q$ denotes the normal vector on the surface. T_n^+ and T_n^- represent two triangles connected to the edge n of the triangulated surface model. $\hat{t}_q^+$ and $\hat{t}_q^-$ are the two unit vectors in the middle of qth edge which are perpendicular to the edge and which are lying the in the plane of the triangle pairs $T_q^{\pm}$. $f_n(\mathbf{r}')$ is the vector basis function. $G(\tilde{\mathbf{r}}, \tilde{\mathbf{r}}')$ is the Green's function in free space defined as

$$G\left(\tilde{\mathbf{r}}, \tilde{\mathbf{r}}'\right) = \frac{e^{-jk|\tilde{\mathbf{r}} - \tilde{\mathbf{r}}'|}}{4\pi\left|\tilde{\mathbf{r}} - \tilde{\mathbf{r}}'\right|} \tag{5}$$

where k denotes the wave number, $\tilde{\mathbf{r}}$ and $\tilde{\mathbf{r}}'$ are the source and observation points, respectively.

2.2. Improved IE-FFT and PO Hybrid Method

In Fig. 1, an improved grids distribution located in the nonempty groups is proposed. By introducing the concept of the empty groups, modified IE-FFT algorithm which is based on the subdomain is employed to reduce matrix storage and to accelerate all the matrix-vector multiplications in both the linear system for the moments and the iterative solver. Furthermore, the correction of the near-interaction is avoided. Note that matrix G is Toeplitz, and this enables the use of FFT to compute the matrix-vector multiplication.

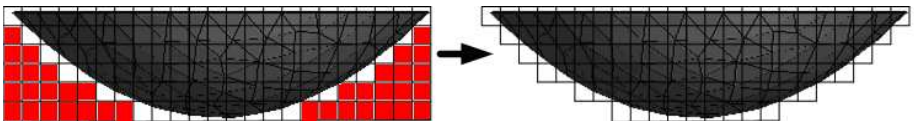

Figure 1. Grid distribution of the improved IE-FFT method.

By interpolating the Green's function on these grids, the matrix equation can be written as

$$\begin{aligned} Z &= Z_{(\text{near})}^{\text{MoM}} + Z_{(\text{far})}^{\text{IE-FFT}} \\ &= Z_{(\text{near})}^{\text{MoM}} + jk_0\eta_0 \left[\alpha \left(\sum_{i=1}^{N} \mathbf{\Pi}_{iA} G_{i,j} \sum_{j=1}^{M_i} (\mathbf{\Pi}_{jA})^T - \frac{1}{k_0^2} \sum_{i=1}^{N} \Pi_{iD} G_{i,j} \sum_{j=1}^{M_i} (\Pi_{jD})^T \right) \right. \\ &\quad \left. - \frac{(1-\alpha)}{jk_0} \sum_{i=1}^{N} \mathbf{\Pi}_{iM} G_{i,j} \sum_{j=1}^{M_i} (\mathbf{\Pi}_{jA})^T \right] \end{aligned} \tag{6}$$

In Equation (6), k_0 and η_0 are wave number and wave impedance of free space, respectively. The projection matrices $\mathbf{\Pi}_A$, Π_D and $\mathbf{\Pi}_M$ are all sparse, and then the matrix vector product can be accelerated by FFT. The projection matrices can be evaluated as follows:

$$\mathbf{\Pi}_A = \int_S \left[f_1(\mathbf{r}), f_2(\mathbf{r}), \ldots, f_N(\mathbf{r}) \right]^T \left[\beta_1(\mathbf{r}), \beta_2(\mathbf{r}), \ldots, \beta_{(p+1)^3}(\mathbf{r}) \right] dS \tag{7}$$

$$\Pi_D = \int_S \left[\nabla \cdot f_1(\mathbf{r}), \nabla \cdot f_2(\mathbf{r}), \ldots, \nabla \cdot f_N(\mathbf{r}) \right]^T \left[\beta_1(\mathbf{r}), \beta_2(\mathbf{r}), \ldots, \beta_{(p+1)^3}(\mathbf{r}) \right] dS \tag{8}$$

$$\mathbf{\Pi}_M = \int_S \left[\nabla f_1(\mathbf{r}), \nabla f_2(\mathbf{r}), \ldots, \nabla f_N(\mathbf{r}) \right]^T \left[\beta_1(\mathbf{r}), \beta_2(\mathbf{r}), \ldots, \beta_{(p+1)^3}(\mathbf{r}) \right] dS \tag{9}$$

$$G_{i,j} = \begin{bmatrix} g_{1,1} & g_{1,2} & \cdots & g_{1,(p+1)^3} \\ g_{2,1} & g_{2,2} & \cdots & g_{2,(p+1)^3} \\ \cdots & \cdots & \cdots & \cdots \\ g_{(p+1)^3,1} & g_{(p+1)^3,2} & \cdots & g_{(p+1)^3,(p+1)^3} \end{bmatrix} \tag{10}$$

where N is the number of panels in a single group i or j. $\beta_i(\mathbf{r})$ are Lagrange interpolation basis functions for nodes i, respectively. p is the approximation order, $(p+1)^3$ is the number of grids. $G_{i,j}$ is a 3-D Toeplitz Green's function matrix produced by the regular grids located in group i or j. $g_{i,j}$ is the Lagrange coefficients of Green's function.

Similar to the above scheme, the hybrid formulation (2) can be derived by decomposing the impedance matrix to near and far field couplings as follows

$$\begin{aligned} \mathbf{Z}_{11} + \mathbf{Z}_{12}\mathbf{A} &= \left[[\mathbf{Z}_{11} + \mathbf{Z}_{12}\mathbf{A}] \right]_{(\text{near})} + \left[\mathbf{Z}_{11} + \mathbf{Z}_{12}\mathbf{A} \right]_{(\text{far})} \\ &= \left[\mathbf{Z}_{11(\text{near})}^{\text{MoM}} + \mathbf{Z}_{12(\text{near})}^{\text{MoM-PO}} \mathbf{A} \right] + \left[\mathbf{Z}_{11(\text{far})}^{\text{IE-FFT}} + \mathbf{Z}_{12(\text{far})}^{\text{IE-FFT}} \mathbf{A} \right] \end{aligned} \tag{11}$$

Using FFT to accelerate the matrix-vector multiplication, we can obtain the following equation

$$\begin{aligned}
\mathbf{V}_1 \;=\; & \left[\mathbf{Z}^{\text{MoM}}_{11(\text{near})} + \mathbf{Z}^{\text{MoM-PO}}_{12(\text{near})}\mathbf{A}\right]\mathbf{I}_1 \\
& + jk_0\eta_0\alpha\left(\sum_{i=1}^{N}\mathbf{\Pi}_{i1A}F^{-1}\left(F(G_{i,j})F\left(\sum_{j=1}^{M_i}(\mathbf{\Pi}_{j1A})^T\mathbf{I}_{1j}\right)\right)\right) \\
& - \frac{j\eta_0}{k_0}\sum_{i=1}^{N}\Pi_{i1D}F^{-1}\left(F(G_{i,j}(k))F\left(\sum_{j=1}^{M_i}(\Pi_{j1D})^T\mathbf{I}_{1j}\right)\right) \\
& - (1-\alpha)\eta_0\sum_{i=1}^{N}\mathbf{\Pi}_{i1M}F^{-1}\left(F(G_{i,j})F\left(\sum_{j=1}^{M_i}(\mathbf{\Pi}_{j1A})^T\mathbf{I}_{1j}\right)\right) \\
& + jk_0\eta_0\alpha\left(\sum_{i=1}^{N}\mathbf{\Pi}_{i1A}F^{-1}\left(F(G_{i,j})F\left(\sum_{j=1}^{M_i}(\mathbf{\Pi}_{j2A})^T\mathbf{A}\mathbf{I}_{1j}\right)\right)\right) \\
& - \frac{j\eta_0}{k_0}\sum_{i=1}^{N}\Pi_{i1D}F^{-1}\left(F(G_{i,j})F\left(\sum_{j=1}^{M_i}(\Pi_{j2D})^T\mathbf{A}\mathbf{I}_{1j}\right)\right) \\
& - (1-\alpha)\eta_0\sum_{i=1}^{N}\mathbf{\Pi}_{i1M}F^{-1}\left(F(G_{i,j})F\left(\sum_{j=1}^{M_i}(\mathbf{\Pi}_{j2A})^T\mathbf{A}\mathbf{I}_{1j}\right)\right) \qquad (12)
\end{aligned}$$

where $\mathbf{\Pi}_{1A}$, Π_{1D} and $\mathbf{\Pi}_{1M}$ are the projection matrices of basis functions in full-wave region. On the other hand, $\mathbf{\Pi}_{2A}$, Π_{2D} and $\mathbf{\Pi}_{2M}$ are those in the asymptotic region. The two operators F and F^{-1} stand for FFT and inverse FFT, respectively.

Once the current vector $\mathbf{I}_1$ in the full-wave region is determined, the vector $\mathbf{I}_2$ can be calculated from Equation (3). It can be seen that the size of matrix equation in (12) is much smaller than that using conventional full-wave algorithm.

2.3. The Best Uniform Approximation Technique

For a given frequency band $k \in [k_a, k_b]$. The coordinate transform is expressed as

$$\tilde{k} = \frac{2k - (k_a + k_b)}{k_b - k_a} \quad \tilde{k} \in [-1, 1] \qquad (13)$$

Then we can obtain the electric current $I_1(k)$ as follows

$$I_1(k) = I_1\left(\frac{\tilde{k}(k_b - k_a) + (k_a + k_b)}{2}\right) \approx \sum_{l=1}^{n} c_l T_l(\tilde{k}) - \frac{c_1}{2} \qquad (14)$$

where

$$c_l \;=\; \frac{2}{n}\sum_{i=1}^{n} I(k_i)T_l\left(\tilde{k}_i\right) \qquad (15)$$

$$\begin{aligned}
T_1\left(\tilde{k}\right) &= 1 \\
T_2\left(\tilde{k}\right) &= \tilde{k} \qquad (16) \\
T_{l+1}\left(\tilde{k}\right) &= 2\tilde{k}T_l\left(\tilde{k}\right) - T_{l-1}\left(\tilde{k}\right) \quad 3 \le l \le n
\end{aligned}$$

To improve the accuracy of the numerical solution, the Chebyshev series in (14) are matched via a rational function. The Maehly approximation for the elements of $I_1(k)$ is

$$I_1(k) \approx R_{LM}\left(\tilde{k}\right) = \frac{P_L\left(\tilde{k}\right)}{Q_M\left(\tilde{k}\right)} = \frac{a_0 T_0\left(\tilde{k}\right) + a_1 T_1\left(\tilde{k}\right) + \ldots a_L T_L\left(\tilde{k}\right)}{b_0 T_0\left(\tilde{k}\right) + b_1 T_1\left(\tilde{k}\right) + \ldots b_M T_M\left(\tilde{k}\right)} \tag{17}$$

where $b_0 = 1$ in common, substitute (17) into (14) and use the identity

$$T_p(x)T_q(x) = \frac{1}{2}\left(T_{p+q}(x) + T_{|p-q|}(x)\right) \tag{18}$$

The unknown coefficients a_i $(i = 0, 1, \ldots, L)$ and b_j $(j = 1, 2, \ldots, M)$ can be obtained as

$$\begin{cases} a_0 = \dfrac{1}{2}b_0 c_0 + \dfrac{1}{2}\displaystyle\sum_{j=1}^{M} b_j c_j \\ a_i = c_i + \dfrac{1}{4}b_i c_0 + \dfrac{1}{2}\displaystyle\sum_{j=1}^{M} b_j\left(c_{j+i} + c_{|j-i|}\right) \\ i = 1, 2, \ldots, L \end{cases} \tag{19}$$

$$\begin{bmatrix} c_{L+2}+c_L & c_{L+3}+c_{L+1} & \ldots & c_{L+M+1}+c_{L-M+1} \\ c_{L+3}+c_{L+1} & c_{L+4}+c_L & \ldots & c_{L+M+2}+c_{L-M+2} \\ \vdots & \vdots & \vdots & \vdots \\ c_{L+M+1}+c_{L+M-1} & c_{L+M+2}+c_{L+M-2} & \ldots & c_{L+2M}+c_L \end{bmatrix} \begin{bmatrix} b_1 \\ b_2 \\ \vdots \\ b_M \end{bmatrix} = -2 \begin{bmatrix} c_{L+1} \\ c_{L+2} \\ \vdots \\ c_{L+M} \end{bmatrix} \tag{20}$$

Once the coefficients of the rational function are calculated, the induced current distribution can be obtained at any frequency within the whole frequency wide-band.

3. NUMERICAL RESULTS

Two numerical examples are considered in this section to illustrate the efficiency and validity of the presented algorithm for solving radiation problems. All the computations are carried out on a PC with Intel Core2 CPU 2.8 GHz and 2G RAM. The data are stored in double precision, and the bi-conjugate gradient stabilized method was employed as iterative solver. In our implementation, the grid distance is 0.08λ and the near-zone threshold d_{near} is 0.4λ. For the Lagrange interpolation operator, the order p is 2 and the coefficient α is 0.8. The methods, such as IEFFT, IEFFT-PO, and IEFFT-PO+Maehly methods, used in the examples are implemented by the Fortran program.

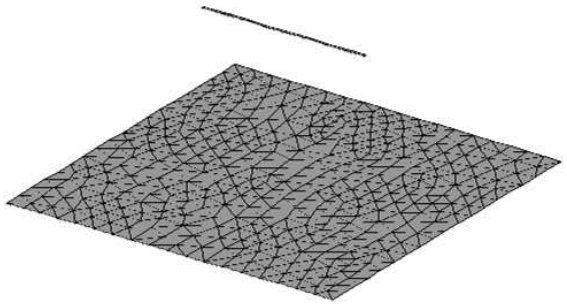

Figure 2. A dipole antenna above a conducting square disk.

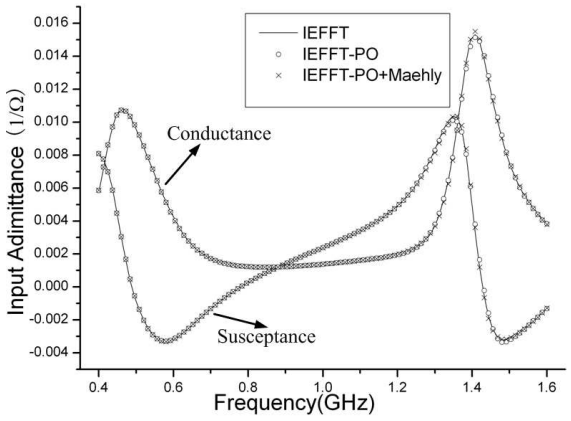

Figure 3. Input admittance frequency response for there methods.

In the first example, we consider a dipole located at a distance of 0.25 m above a conducting square disk, as shown in Fig. 2. The height of the dipole is 0.3 m, and the size of the disk is 0.6 m × 0.6 m. In the hybrid analysis, the dipole is assigned to the full-wave region, with the square being the PO region. There are 15 basis functions in the full-wave region while 1089 basis functions are in the PO region. Fig. 3 shows the input admittance response from 0.4 to 1.6 GHz obtained using IEFFT, IEFFT-PO, and IEFFT-PO+Maehly methods. The frequency step is 12 MHz and 101 frequency points are used for the frequency response. It can be seen that the result from the IEFFT-PO and Maehly hybrid method agrees exactly with that from the conventional IEFFT. In Fig. 4, the results of radiation pattern in the plane of $\varphi = 0^\circ$ calculated by the hybrid algorithm are also in agreement with the conventional method unless some deviations are due to the fact that the edge diffraction field, which is the largest portion of the fields behind the square, was not taken into account. This example shows that it is viable to apply our hybrid technique to analyze the radiation of antennas around a conducting platform.

The second example considered in this paper is an antenna array located at a distance of 0.3 m above a parabolic reflector, as shown in Fig. 5. The diameter and focal length of the parabolic reflector is 1 m and 0.8 m, The four elements in the array are bowtie antenna whose size is shown in the picture. The array operate at a frequency of 1 GHz. In the simulation, four bowtie antennas are assigned to the full-wave region with the parabolic reflector being the PO region. Fig. 6 shows the input admittance response from 0.4 to 1.6 GHz obtained using IEFFT, IEFFT-PO, and IEFFT-PO+Maehly methods. Fig. 7 shows that the results of radiation pattern in the plane of $\varphi = 0^\circ$ calculated by the hybrid method agree exactly with that from the conventional IEFFT and the commercial EM software FEKO 6.0. Computational characteristics of the four methods are summarized in Table 1. It can be seen that applying the IEFFT-PO and Maehly hybrid method results in a reduction of the number of unknowns and near field couplings. Therefore, the CPU time are drastically reduced. It should be noted that the memory overflow occurs in the PC with the asymptotic waveform evaluation technique in this example. Table 1 shows the efficiency of our hybrid method when it is applied to solve the electrically large problems. It should be noted that the IEFFT method can be applied when the accuracy of results is the main target in the project. However, when the efficiency is the main target, the IEFFT-PO and Maehly hybrid method should be chosen firstly.

The relative root mean square (RMS) RCS error of a specific object is calculated by

$$\text{Error}_{\text{RMS}} = \left[\frac{1}{N} \sum_{j=1}^{N} \left| 10 \log_{10} \left(\frac{\tilde{\sigma}_j(\theta)}{\sigma_j(\theta)} \right) \right|^2 \right]^{1/2} \tag{21}$$

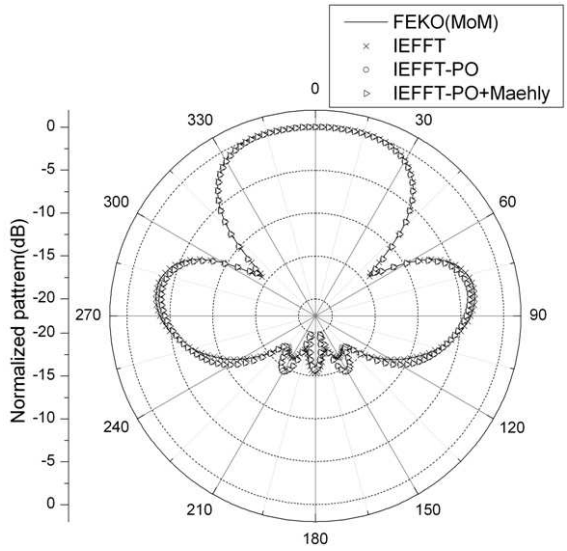

Figure 4. Radiation pattern of $\varphi = 0^\circ$ plane in example 1.

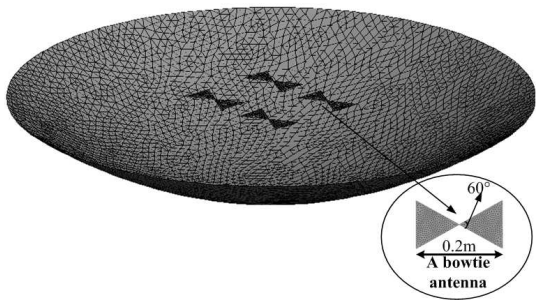

Figure 5. An antenna array above a circular disk.

Table 1. Computational characteristics of the four methods for Fig. 5.

Method	No. of unknowns	No. of near field couplings	Total CPU time (hours)
IEFFT	11854	4680725	150
IEFFT-PO	1284	380742	64
IEFFT-PO+Maehly	1284	103237	20.5
FEKO (MoM)	11854	None	40

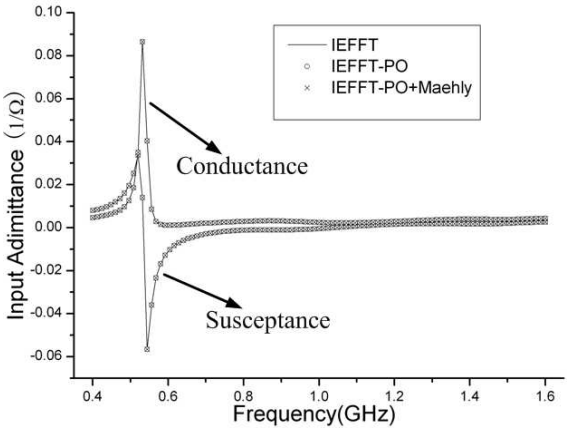

Figure 6. Input admittance frequency response for there methods.

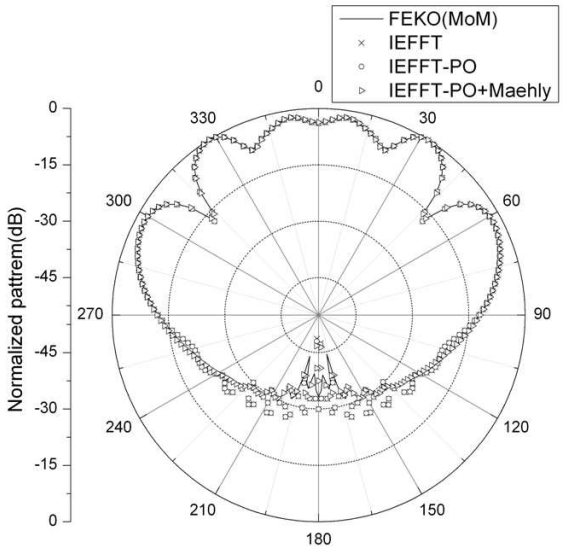

Figure 7. Radiation pattern of $\varphi = 0^\circ$ plane in example 2.

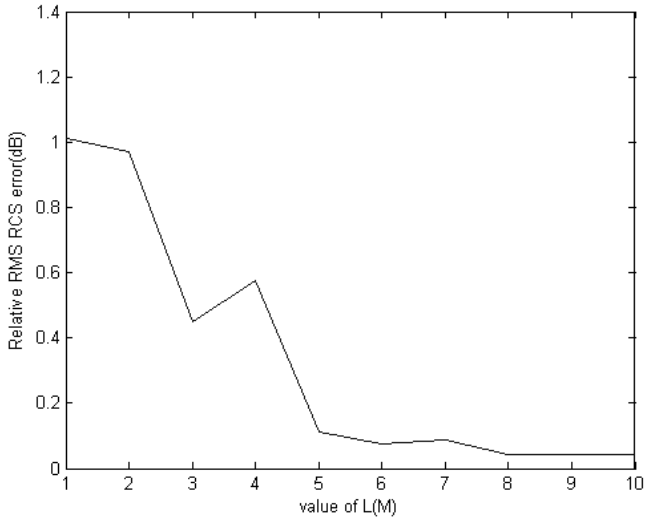

Figure 8. Relative RMS RCS error with the value of $L(M)$.

where N represents selected frequency points, while $\tilde{\sigma}_j(\theta)$ and $\sigma_j(\theta)$ are the RCS obtained by the proposed method and the IEFFT-PO method, respectively. For the second example, Fig. 8 shows that while the expanded coefficient $L(M)$ is greater than 8, the relative RMS RCS error is less than 0.05 dB.

4. CONCLUSION

An IE-PO hybrid method in conjunction with the best uniform approximation technique has been presented to obtain fast frequency sweep response of antennas around electrically large platform. The improved IE-FFT scheme based on subdomains is described, which can reduce memory requirements and avoid the correction of near-interactions. After hybridizing PO approach, the algorithm can well handle electrically large problems. Since the IE-PO algorithm requires $O(N^{1.5})$ for storage, there is still an electrical size limit in the proposed method. The limitation depends on the region assignment and the number of unknowns in the full-wave region. In practice, the full-wave region is usually smaller than the PO region. The fact makes that the IE-PO can be utilized to analyze antennas mounted on a very large platform such as planes and ships. Furthermore, the best uniform approximation technique is utilized to achieve fast frequency sweeping. Finally, numerical results show the validity and efficiency of the method proposed in this paper and that the unknowns and the calculation time are about 1/7 and 1/9 of what needed in the original method.

ACKNOWLEDGMENT

This work was supported by the National Natural Science Foundation of China (No. 61201023) and the Fundamental Research Funds for the Central Universities (K5051302021).

REFERENCES

1. Jakobus, U. and F. M. Landstorfer, "Improved PO-MM hybrid formulation for scattering from three-dimensional perfectly conducting bodies of arbitrary shape," *IEEE Trans. Antennas Propagat.*, Vol. 43, No. 2, 162–169, 1995.
2. Obelleiro, F., J. M. Taboada, J. L. Rodríguez, J. O. Rubiños, and A. M. Arias, "Hybrid moment-method physical-optics formulation for modeling the electromagnetic behavior of on-board antennas," *Microw. Opt. Technol. Lett.*, Vol. 27, No. 2, 88–93, Oct. 2000.
3. Ma, J., S. X. Gong, X. Wang, et al., "Efficient IE-FFT and PO hybrid analysis of antennas around electrically large platforms," *IEEE Antennas and Wireless Propagation Letters*, Vol. 10, 611–614, 2011.
4. Song, J. M. and W. C. Chew, "Multilevel fast multipole algorithm for solving combined field integral equation of electromagnetic scattering," *Microw. Opt. Technol. Lett.*, Vol. 10, No. 1, 14–19, Sep. 1995.
5. Song, J. M., C. C. Lu, and W. C. Chew, "Multilevel fast multipole algorithm for electromagnetic scattering by large complex objects," *IEEE Trans. Antennas Propagat.*, Vol. 45, No. 10, 1488–1493, Oct. 1997.
6. Song, J. M. and W. C. Chew, "Fast multipole method solution of combined field integral equation," *11th Annual Review of Orogress in Applied Computational Electromagnetics*, Vol. 1, 629–636, Monterey, California, Mar. 1995.
7. Rokhlin, V., "Rapid solution of integral equations of classical potential theory," *J. Comput. Phys.*, Vol. 60, 187–207, 1985.
8. Coifman, R., V. Rokhlin, and S. Wandzura, "The fast multipole method for the wave equation: A pedestrian prescription," *IEEE Antennas Propagat. Mag.*, Vol. 35, No. 3, 7–12, Jun. 1993.
9. Phillips, J. R. and J. K. White, "A precorrected-FFT method for electrostatic analysis of complicated 3-D structures," *IEEE Trans. Computer-Aided Design Integr. Circuits Syst.*, Vol. 16, No. 10, 1059–1072, Oct. 1997.
10. Phillips, J. R., "Error and complexity analysis for a collocation grid projection plus precorrected-FFT algorithm for solving potential integral equations with Laplace or Helmholtz kernels," *Proc. 1995 Copper Mountain Conf. Multigrid Methods*, 673–688, Apr. 1995.
11. Bleszynski, E., M. Bleszynski, and T. Jaroszewicz, "AIM: Adaptive integral method for solving large-scale electromagnetic scattering and radiation problems," *Radio Sci.*, Vol. 31, No. 5, 1225–1251, 1996.

12. Wang, C. F., F. Ling, J. M. Song, and J. M. Jian, "Adaptive integral solution of combined field integral equation," *Microw. Opt. Technol. Lett.*, Vol. 19, No. 5, 321–328, 1998.
13. Seo, S. M. and J. F. Lee, "A fast IE-FFT algorithm for solving PEC scattering problem," *IEEE Transactions on Magnetics*, Vol. 41, No. 5, 1476–1479, 2005.
14. Ma, J., S. X. Gong, X. Wang, Y. Liu, and Y. X. Xu, "Efficient wide-band analysis of antennas around a conducting platform using MoM-PO hybrid method and asymptotic waveform evaluation technique," *IEEE Trans. Antennas Propagat.*, Vol. 60, No. 12, 6048–6052, 2012.
15. Peng, Z. and X. Q. Sheng, "A bandwidth estimation approach for the asymptotic waveform evaluation technique," *IEEE Trans. Antennas Propagat.*, Vol. 56, No. 3, 913–917, 2008.
16. Nie, X. C., N. Yuan, L. W. Li, and Y. B. Gan, "Fast analysis of RCS over a frequency band using pre-corrected FFT/AIM and asymptotic waveform evaluation technique," *IEEE Trans. Antennas Propagat.*, Vol. 56, No. 11, 3526–3533, 2008.
17. Wang, X., S. X. Gong, J. L. Guo, Y. Liu, and P. F. Zhang, "Fast and accurate wide-band analysis of antennas mounted on conducting platform using AIM and asymptotic waveform evaluation technique," *IEEE Trans. Antennas Propagat.*, Vol. 59, No. 12, 4624–4633, 2011.
18. Güdü, T. and L. Alatan, "Use of asymptotic waveform evaluation technique in the analysis of multilayer structures with doubly periodic dielectric gratings," *IEEE Trans. Antennas Propagat.*, Vol. 57, No. 9, 2641–2649, 2009.
19. Burke, G. J., E. K. Miller, S. Chakrabarthi, et al., "Using model-based parameter estimation to increase the efficiency of computing electromagnetic transfer functions," *IEEE Transactions on Magnetics*, Vol. 25, No. 7, 2807–2809, Jul. 1989.
20. Hernandez, M. A., "Chebyshev's approximation algorithms and applications," *Computers & Mathematics with Applications*, Vol. 41, No. 3–4, 433–455, 2001.
21. Chen, M. S., X. L. Wu, Z. X. Huang, and W. Sha, "Accurate computation of wideband response of electromagnetic scattering problems via Maehly approximation," *Microw. Opt. Technol. Lett.*, Vol. 49, No. 5, 1144–1146, 2007.
22. Chen, M. S., X. L. Wu, W. Sha, and Z. X. Huang, "Fast and accurate radar cross-section computation over a broad frequency band using the best uniform rational approximation," *IET Microw. Antennas Propag.*, Vol. 2, 200–204, Feb. 2008.